Fuel 345 (2023) 128198

Contents lists available at ScienceDirect

Fuel

journal homepage: www.elsevier.com/locate/fuel

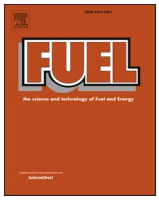

Aqueous formate solution for enhanced water imbibition in oil recovery and carbon storage in carbonate reservoirs

Hao Wang, Oluwafemi Precious Oyenowo, Ryosuke Okuno *

Hildebrand Department of Petroleum and Geosystems Engineering, The University of Texas at Austin, Austin, TX 78712, USA

ARTICLE INFO

Keywords:
Formate
Wettability alteration
Carbon sequestration
Water imbibition
Carbonate formation
Enhanced oil recovery

ABSTRACT

This paper presents an experimental study of the injection of aqueous formate solution into oil-wet carbonate porous media at different formate concentrations and acidity levels. The research was motivated by the potential use of aqueous formate solution as a wettability modifier in enhanced oil recovery and/or a carbon carrier in geological carbon storage in carbonate reservoirs. However, the wettability alteration of carbonate rocks by formate has not been tested at elevated concentrations of formate or in any coreflood. The experimental program in this research consists of aqueous stability, wettability alteration, and three dynamic imbibition experiments with fractured carbonate cores with varying formate concentrations up to 30 wt% and initial pH between 6 and 7.

With an excess amount of calcite powder, the 20 wt% formate solution in 15000 ppm NaCl brine showed essentially the same pH history as the base NaCl brine, where calcite dissolution caused the solution pH to increase to a stable value near 9. None of the samples studied in this research showed solid precipitation. Material balance of dynamic imbibition data indicated that the imbibition of formate into the matrix was most significant in coreflood #1, in which 30 wt% formate solution was injected into a fractured carbonate core. A large gradient in formate concentration between the fracture and the matrix likely caused the rapid mass transfer. Then, calcite dissolution and the resulting formate species caused wettability alteration to enhance water imbibition, which in turn expelled the oil in the matrix.

The incremental oil recovery factor was 9.1 % for 30 wt% formate (pH = 7; coreflood #1), 2.9 % for 5 wt% formate (pH = 7; coreflood #2), and 7.0 % for 5 wt% formate + HCl (pH = 6; coreflood #3). A greater oil recovery factor resulted from a greater concentration of formate and a reduced pH. This is the first time corefloods were performed with aqueous formate solution at elevated concentrations up to 30 wt%.

1. Introduction

This section first gives a discussion of the technical challenges for carbon capture and storage (CCS) in carbonate reservoirs and then discusses several ways to improve the efficiency of oil recovery and CCS in carbonate reservoirs. Finally, the research objectives of this paper are introduced.

Carbonate reservoirs account for approximately 60 % of the world's crude oil and natural gas reserves [1,2]. Waterflooding and gas flooding are widely used to develop carbonate reservoirs, and 67 % of CO_2 floods in the U.S. are in carbonate reservoirs [3]. However, carbonate reservoirs usually contain multiscale natural fracture networks, causing large fluid-mobility contrasts between high-permeability fractures and low-permeability matrices to make the oil recovery inefficient. Therefore, improving the sweep efficiency in carbonate reservoirs has been studied over the past few decades [4,5].

Carbonate reservoirs are also considered for CCS, in which a large amount of carbon can be stored while improving oil recovery [6–8]. However, CO_2 storage in carbonate reservoirs depends on the in-situ flow regime of CO_2, which tends to result in inefficient volumetric sweep because of the channeling flow of CO_2 through high-permeability fractures in heterogeneous carbonate reservoirs [9]. For example, CO_2 flooding was performed in the east portion of East Seminole Field, which is a heterogeneous carbonate reservoir in the Permian Basin, in 2013. However, a rapid CO_2 breakthrough with large gas-oil ratios (GOR) was soon observed because of the channeling flow [10]. Lv et al. [11] used $CaCO_3$-coated micromodels to study the sweep efficiency of CO_2 injection into heterogeneous carbonate porous media. They found that many

* Corresponding author.
E-mail address: okuno@utexas.edu (R. Okuno).

https://doi.org/10.1016/j.fuel.2023.128198
Received 5 November 2022; Received in revised form 11 March 2023; Accepted 22 March 2023
Available online 29 March 2023

branches of CO_2 flow were formed in the fractures and pores, leading to a low sweep efficiency of 28.1 %. Since the viscosity of CO_2 is low in comparison to brine and oil at reservoir temperature and pressure, the mobility ratio in CO_2 injection is usually unfavorable in saline aquifers and oil reservoirs. The high mobility of the injection gas, CO_2, exacerbates the volumetric sweep with a large permeability contrast in carbonate reservoirs [12]. In addition, the gravity override, which resulted from the low density of CO_2, drives CO_2 to rise toward the caprock. CO_2 leakage may occur when the caprock is not fully impermeable to CO_2 with or without hydraulic paths, such as faults, fractures, and wellbores. Complex geochemical reactions during CCS in carbonate reservoirs should be also studied for deposition of minerals (e.g., calcite, magnesite), which may plug pores and tubings [9].

In addition to the in-situ flow regime in CO_2 injection, the rock wettability in carbonate reservoirs can make it difficult for CO_2 to transfer from high-permeability fractures to low-permeability matrices. Calcite in carbonate reservoirs tends to be oil- or mixed-wet in the presence of polar components in the oil, such as naphthenic acids [13]. For the same reason, waterflooding in carbonate reservoirs can be challenging because water imbibition into oil-wet carbonate matrices is weak [14,15].

One way to improve the efficiency of oil recovery and CCS in carbonate reservoirs is to use wettability alteration in water-based enhanced oil recovery (EOR). Hirasaki [16] pointed out that the wettability of rock surfaces could be changed from oil-wet to water-wet by increasing the stability of the water film or removing the polar components absorbed on the rock surfaces. Surfactants have been widely studied for wettability alteration for carbonate formations [17–19]. Cationic surfactants were effective in altering the wettability of carbonate rock surfaces from oil-wet to water-wet, in which the positively charged head of surfactants paired with negatively charged carboxylate acids that were absorbed on the rock surface by electrostatic interaction [20]. The ion pair was able to remove the absorbed organic components on the rock surface and contributed to the wettability alteration. Anionic surfactants were less effective in wettability alteration than cationic surfactants because the wettability alteration by anionic surfactants was considered reversible [21]. The proposed mechanism was that a bilayer structure was formed by the hydrophobic interactions between the hydrophobic tails of surfactant and the absorbed organic components, which decreased the contact angle and altered the wettability. Although surfactants were an effective wettability modifier, the reduced IFT between water and oil reduced the kinetics of water imbibition [22]. Also, various wettability modifiers are less expensive than surfactants.

Low-salinity waterflooding has been widely investigated for wettability alteration [23–25]. The mechanisms of wettability alteration by low-salinity waterflooding were reviewed by Sheng [26], including multicomponent ion exchange [27] and electrical double layer expansion [28]. Hiorth et al. [29] concluded that calcite dissolution was also an important mechanism for wettability alteration in carbonate reservoirs. They found a positive correlation between the percentage of calcite dissolution and the oil recovery. When calcite dissolution occurred where oil was absorbed, the oil would be removed, rendering the rock surface less oil-wet. Den Ouden et al. [30] also attributed the mechanism of wettability alteration to calcite dissolution. They observed the increased concentration of calcium and pH after the equilibrium between crushed calcite material and low-salinity water. The pH increased because CO_3^{2-} was generated from dissolved calcite. They also indicated that the effect of calcite dissolution was more significant with increasing CO_2 partial pressure and decreasing pH. The increased concentration of Ca^{2+} and pH of effluent samples were important indicators for calcite dissolution and, therefore, wettability alteration.

More recently, Baghishov et al. [31] presented the wettability alteration of carbonate rocks by aqueous formate solutions. They conducted contact angle experiments and Amott tests with aqueous formate solutions with/without pH adjustment by hydrogen chloride (HCl). Results showed that aqueous formate solution was effective in altering the wettability of oil-wet carbonate rocks to a water-wet state when the initial solution pH was adjusted to 6.1. They proposed that the mechanisms of wettability alteration by formate were the calcite dissolution and adsorption of formate on the rock surface. However, they only tested the wettability alteration with at most 5 wt% formate in brine, and they did not perform coreflooding experiments. A coreflooding experiment enabled them to evaluate the lab-scale oil displacement and rock-fluid interactions when formate solution was injected into a core. Since formate species can be used in CCS as a highly water-soluble carbon carrier [32], important questions arise as to how the wettability alteration would occur with an elevated concentration of formate, and how the carbon carrier (i.e., formate) would transfer to the carbonate rock matrix in response to the expected wettability alteration. These questions motivated this research.

In this research, aqueous formate solutions with high concentrations of formate were investigated, not only as a wettability modifier, but also as a carbon carrier, for EOR and/or CCS in carbonate formations. Oyenowo et al. [32] presented the solubility and viscosity data for aqueous formate solutions. Their numerical simulation indicated that the injection of aqueous formate solution led to a greater amount of oil recovery and carbon storage mainly because aqueous formate solution stabilized the displacement fronts. Okuno [33] presented that when the mass density of pure CO_2 at bottom-hole conditions was smaller than 9 mol/L, the carbon density in aqueous formate solution was greater than that of CO_2, and a greater carbon injection rate was expected by aqueous formate solution than CO_2 for a given well-head pressure. However, it is not clear how a high-concentration formate solution would interact with carbonate rocks in formate-based EOR and/or CCS.

The main goal of this paper is to investigate the wettability alteration of aqueous formate solutions for oil-wet carbonate porous media at different formate concentrations and acidity levels. The stability test was conducted by aqueous formate solutions with and without calcite powder. The pH history was recorded during the aging period. Wettability alteration was studied with oil-aged calcite plates and cores. Three dynamic imbibition experiments were carried out with 30 wt% formate solution with a pH of 7, 5 wt% formate solution with a pH of 7, and 5 wt % formate solution with a pH of 6 to investigate how the formate concentration and the solution pH would affect the wettability alteration. Results were analyzed by material balance, which quantitatively indicated the mass transfer between the fracture and matrix volumes in the corefloods.

In what follows, section 2 presents the material and methods for this research. Section 3 gives the main results of aqueous stability, wettability alteration, and coreflooding, followed by comparative discussions. Section 4 shows the main conclusions from this research.

2. Material and methods

This section presents the experimental conditions and procedures. The experiments include measurement of fluid properties, stability test, wettability alteration test, and dynamic imbibition experiments.

2.1. Fluid properties

This study used an oil sample from a conventional oil reservoir in Texas. Table 1 shows the density and viscosity measured at room temperature and atmospheric pressure. All experiments used 15000-ppm

Table 1
Properties of the oil sample.

Density, kg/m^3	795 (at 295 K)
Viscosity, Pa·s	2.7×10^{-3} (at 295 K)
Molecular weight, g/mol	183

NaCl brine with a pH of 7, which had a mass density of 1004 kg/m^3.

Sodium formate (Thermo Scientific, purity: 99 %) was used to provide formate ion for the aqueous solutions. The pH of formate solutions was adjusted to 7 by adding formic acid (HCOOH). The amount of formic acid added to the solution was based on the Henderson-Hasselbalch equation

$$pH = pK_a + \log_{10}\left(\frac{[HCOO^-]}{[HCOOH]}\right) \quad (1)$$

where pH is the acidity of the formate/formic acid buffer solution; pK_a is the negative logarithm of the acid dissociation constant; $[HCOO^-]$ is the molar concentration of formate, mol/L; [HCOOH] is the molar concentration of formic acid, mol/L. The calculation used a pK_a value of 3.75 at 25 °C.

This study used two formate concentrations in brine, 5 wt% and 30 wt%. The total salinity is 90556 ppm (Na^+: 31459 ppm, Cl^-: 9097 ppm, $HCOO^-$: 50000 ppm) and 468333 ppm (Na^+: 159236 ppm, Cl^-: 9097 ppm, $HCOO^-$: 300000 ppm), respectively. Figs. 1 and 2 show the measured viscosities and densities of formate solutions. The densities and viscosities were measured for three times for each sample to ensure the repeatability of the measurement. All experimental values of triplicate measurements were within 9 % of the further used averages.

2.2. Stability test

The NaCl brine and the formate solutions were prepared for stability testing as shown in Table 2. The thermal stability was tested using 20 wt % formate in brine. The other two solutions were used for studying the stability of formate solutions with calcite and any reaction that exists. The same amount of calcite powder was added to these two solutions, and the solution pH was adjusted to 7 by adding formic acid as mentioned previously. The glass chamber had a sealing to minimize the loss of water by evaporation. Then, the solutions were placed in an oven at 85 °C for over 30 days. During this process, the pH of each solution was recorded every-five days. The calcite levels in the sample bottles were also observed.

2.3. Wettability alteration test

Wettability alteration tests had two parts: the first part used calcite plates and the second part used disk-shaped cores. They were performed at room temperature to identify the wettability alteration by formate solutions. The 15000-ppm NaCl brine was used for the control experiment. To investigate the effect of formate concentration on wettability alteration, 30 wt% and 5 wt% formate solutions were used. A fourth case

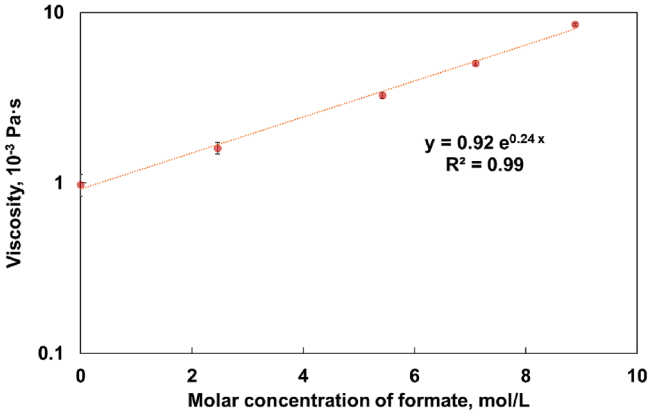

Fig. 1. Measured viscosities and a correlation between viscosity and molar concentration of formate based on the measured data. Note that the formate solution is a Newtonian fluid and therefore, the formate solution viscosity is independent of shear rate.

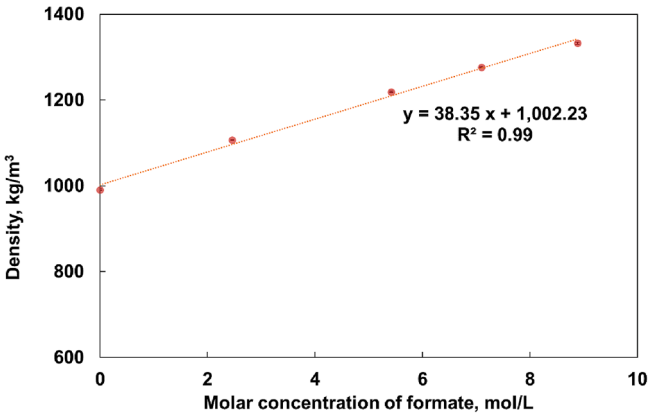

Fig. 2. Measured densities and a correlation between the density and molar concentration of formate based on the measured data.

Table 2
Solutions for stability test.

Base brine	Solutions
15000 ppm NaCl	20 wt% formate in brine Brine + calcite 20 wt% formate in brine + calcite

was to test the impact of the solution pH as done by Baghishov et al. [31], in which HCl was added to 5 wt% formate solution while stirring slowly to reach a pH value of 6.

Calcite plates were polished to make the surface smooth. Then, the air-dried calcite plates were aged in the brine for one day at 70 °C. Next, the brine-aged calcite plates were aged in heavy oil for two weeks at 85 °C to make the calcite surfaces more oil-wet. After the aging, calcite plates were retrieved from the glass chamber, and the excess oil on the surface was removed carefully. The oil-aged calcite plates were placed on a stand in the glass chamber filled with formate solutions. The glass chambers were tightly closed and placed at room temperature. Photos of surface of calcite plates were taken regularly after the initialization of the experiment.

In addition to calcite plates, wettability alteration was tested with Texas Cream limestone with a diameter of 2.54 cm. The permeability and porosity of the core were measured to be 15.5 mD and 31.8 %, respectively. Then, it was aged in oil for at least one month at 70 °C. After that the core was cut into pieces with a thickness of 1 cm. To start the experiment, the disk-shaped cores were immersed in the four different solutions. The rock surfaces wet by oil were monitored regularly after the initialization of the experiment.

2.4. Dynamic imbibition experiments

A total of three dynamic imbibition experiments were conducted with 30 wt% formate solution (Coreflood #1), 5 wt% formate solution (Coreflood #2), and 5 wt% formate + HCl solution (Coreflood #3). Corefloods #1 and #2 were to see the effect of the formate concentration on wettability alteration, and Corefloods #2 and #3 were to see the effect of pH. Corefloods #1 and #3 were to see which would result in more effective wettability alteration, increasing the formate concentration or adjusting the formate solution pH as suggested by Baghishov et al. [31].

Texas Cream limestones were used for the experiments. The dimensions of the cores were 2.54 cm in diameter and 22.86 cm in length. Core #2 was cut to 20.32 cm because of the dimensions of the core holder used for Coreflood #2. The porosities and permeabilities of the cores were measured with the NaCl brine.

Oil was injected into the cores to establish the initial oil saturation at

room temperature. The injection rate was fixed at 30 cm^3/hour before the oil breakthrough and then changed to 50 cm^3/hour to minimize the capillary-end effect with a capillary number of 2.3 × 10^{-5} and a Rapoport and Leas number (N_{RL}) of 10.15 cm^2·cp/min. According to Rapoport and Leas [34], the capillary-end effect was negligible when the scaling coefficient Luμ (N_{RL}) was greater than 0.5–3.5 cm^2·cp/min, in which L is the length of the core, u is the injection rate, and μ is the viscosity of the injected solution. The injection of oil was continued until the amount of produced water became negligible. The initial oil saturation was quantified by the total production volume of brine. After that, the oil-saturated cores were aged in crude oil for at least one month at 70 °C. The cores were oil flooded again after the aging since the initial water saturation could be changed slightly by wettability alteration.

An electric saw created an artificial fracture along the longitudinal direction for each core. Two Teflon strips of 0.1 cm in width and 22.86 cm (20.32 cm for Core #2) in length were placed inside the fracture to keep the aperture of the fracture. Then, the cores were wrapped with a shrinkable polytetrafluoroethylene (PTFE) tube as shown in Fig. 3. Finally, the cores were placed inside the core holder with the fracture vertically oriented to control the gravity effect on oil displacement [35].

The fractured core was oil flooded again to make the fracture volume fully saturated by oil. The valve at the outlet of the core holder was partially closed to make sure the oil filled out the fracture volume. The fracture/matrix permeability ratio was set to be between 30,000 and 40,000 for three dynamic imbibition experiments. The fracture permeability was measured with oil by adjusting the overburden pressure. Then, the fracture aperture was calculated by the analytical equation [36]:

$$b = (3\pi d k_e)^{\frac{1}{3}} \tag{2}$$

where b is the fracture aperture, m; d is the diameter of the core, m; k_e is the effective oil permeability of the fractured core, D. The fracture permeability was calculated by the following equation [36]:

$$k_f = \frac{b^2}{12} \tag{3}$$

Table 3 lists the properties of three cores. The flow capacity was the product of permeability and cross-sectional area. The initial matrix oil saturation was similar for three cases and was close to reported oil saturation values for Texas Cream limestone [37]. One important factor that affects the capillary pressure is the pore radius, which can be calculated by the following equation:

$$r = \sqrt{\frac{8k}{\varphi}} \tag{4}$$

Fig. 3. Artificially fractured cores wrapped with a PTFE tube.

Table 3
Properties of the cores used for dynamic imbibition experiments. The unit of permeability is millidarcy (mD).

	Core #1	Core #2	Core #3
Matrix porosity, %	30.8	28.7	28.4
Matrix permeability, mD	19.64	16.59	13.51
Matrix water saturation	0.361	0.345	0.351
Matrix oil saturation	0.639	0.655	0.649
Flow capacity of the matrix, m^4	9.90×10^{-18}	8.37×10^{-18}	6.82×10^{-18}
Mass of the core before cutting, g	246.17	221.92	251.40
Mass of the core after cutting, g	224.84	200.5	227.79
Matrix pore volume after cutting, cm^3	32.47	26.49	29.69
Overburden pressure, kPa	1516	689	4826
Fracture aperture, μm	97.5	81.1	80.9
Fracture permeability, D	792	548	546
Permeability contrast between fracture and matrix	40,336	33,022	40,427
Flow capacity of fracture, m^4	1.96×10^{-15}	1.13×10^{-15}	1.12×10^{-15}
Fracture pore volume, cm^3	0.564	0.419	0.468
Total pore volume, cm^3	33.03	26.91	30.16

where k is the permeability and φ is the porosity of the matrix. The calculated average pore radii for three cores are 22.59, 21.50 and 19.51 μm, which result in capillary pressures on the same order of magnitude. Therefore, the imbibition rate and oil recovery are mainly affected by wettability alteration by formate solutions.

Dynamic imbibition experiments were performed at room temperature using the setup shown in Fig. 4. It consisted of a pressurization pump, three accumulators for reservoir brine, oil and formate solution, a core holder, a hydraulic manual pump, a pressure gauge, and graduated cylinders for collecting effluent samples.

First, the NaCl brine was injected at 3 cm^3/hour for about 1.0 PVI. For the second stage, formate solution was injected for approximately 1.0 PVI. The flow rate for the formate solution stage was determined by 5 h of residence time in the fracture volume:

$$\tau = \frac{V_f}{q} \tag{5}$$

where τ is the residence time of formate in the fracture volume, hour; V_f is the fracture volume, cm^3; q is the injection rate of formate solution, cm^3/hour. The 5 h of residence time is longer than some reported values to accommodate a period of time for the expected dissolution of calcite [38].

A substantial level of the transverse mass transfer happened for the formate solution flowing in the fracture and directly affected the wettability and oil recovery. Damkhöler number (N_{Da}) is the ratio of characteristic times for transverse mass transfer and longitudinal convection, as calculated by

$$N_{Da} = \frac{KL}{u} \tag{6}$$

where K is the mass-transfer coefficient, s^{-1}; L is the length of the core, m; *u* is the fluid velocity in the fracture, m/s [39]. Note that L/u in equation (6) is the residence time, which is 5 h for the three cases. Therefore, the Damköhler number in the three experiments depends only on K, which is affected by the rock wettability.

Finally, the chase brine was injected at the same flow rate as the formate solution stage until the end of the experiment. Table 4 summarizes the injection schemes for three cases.

The effluent samples were collected in plastic graduated vials. The pH value of aqueous phase was measured by a pH meter as an indicator for calcite dissolution. The formate concentrations for the formate stage and the chase brine stage were measured by proton nuclear magnetic resonance (^{1}H NMR). The concentration data were used for the material balance analysis (Section 2.5). The concentration of Ca^{2+} in the effluent

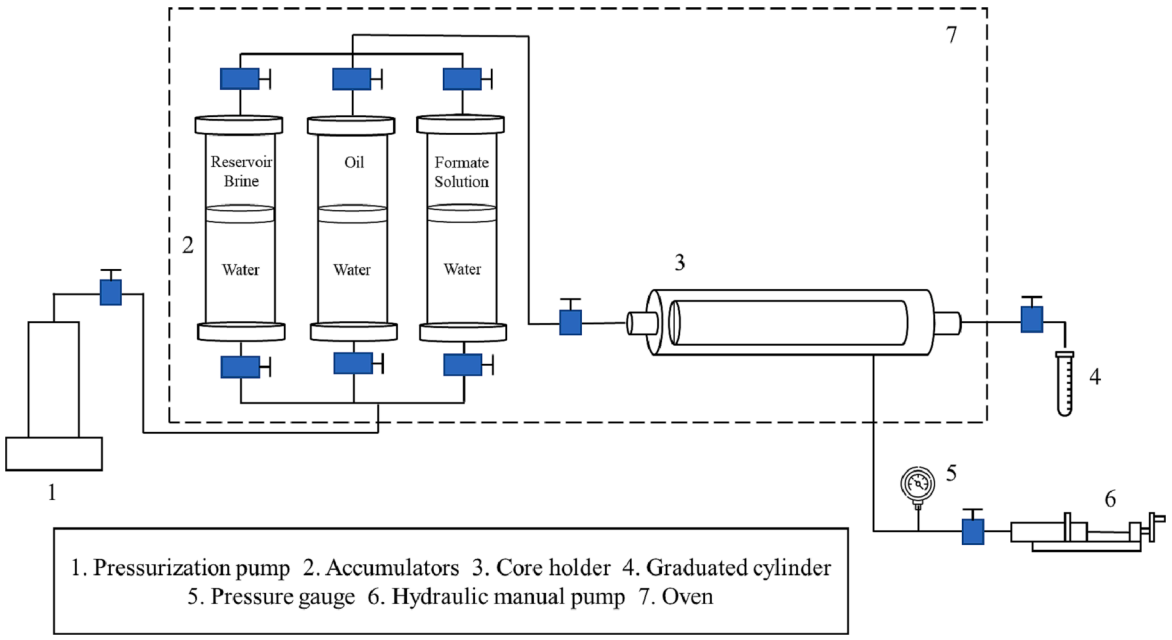

Fig. 4. Experimental setup for dynamic imbibition experiments.

Table 4
Injection schemes for dynamic imbibition experiments.

	Core #1	Core #2	Core #3
Brine stage	Reservoir brine (15000 ppm NaCl, pH = 7) was injected at 3 cm^3/hr for about 1 PVI		
Formate stage	Case 1: 30 wt% formate solution (pH = 7) was injected at 0.11 cm^3/hr for about 1 PVI	Case 2: 5 wt% formate solution (pH = 7) was injected at 0.085 cm^3/hr for about 1 PVI	Case 3: 5 wt% formate + HCl solution (pH = 6) was injected at 0.1 cm^3/hr for about 1 PVI
Chase brine stage	Case 1: Reservoir brine was injected at 0.11 cm^3/hr	Case 2: Reservoir brine was injected at 0.085 cm^3/hr	Case 3: Reservoir brine was injected at 0.1 cm^3/hr

sample was measured by inductively coupled plasma mass spectrometry (ICP-MS).

2.5. Material balance analysis

The material balance for dynamic imbibition experiments with fractured cores was used to analyze the mass transfer between fracture and matrix as in Argüelles-Vivas et al. [37]. This section presents the main procedure of the material balance analysis.

Three components considered in the material balance analysis were brine, oil, and formate. The system consists of two sub-volumes: fracture and matrix. Only the fracture volume is connected to an inlet (injector) and an outlet (producer), and any mass transfer between the two sub-volumes occurs via the fracture-matrix interface. Other assumptions include constant temperature and no effect of calcite dissolution on the material balance for the three components considered in the analysis. Although calcite dissolution will induce species, such as Ca^{2+} and CO_3^{2-}, the focus of the analysis is on the main (pseudo) components, brine, oil, and formate in this paper. Details of aqueous speciation require additional experiments and therefore, they are outside the scope of the current paper.

Three components are labeled as follows: component 1 for brine, 2 for oil, and 3 for formate. The mass balance equations for a given time interval Δt are

$$\Delta M_{fi} = M_{ti} + M_{Ii} + M_{Pi} \tag{7}$$

$$\Delta M_{mi} = -M_{ti} \tag{8}$$

for the fracture and matrix volumes, respectively. ΔM_{fi} and ΔM_{mi} are the change in mass for component i in the fracture and matrix volumes, respectively. M_{ti} is the net mass transfer from the matrix to the fracture for component i. M_{Ii} and M_{Pi} are the mass of component i going into the fracture from the injector and producer, respectively. Fig. 5 shows the mass balance for dynamic imbibition. The positive direction goes from the matrix to the fracture volume.

Under the assumption of steady state flow in the fracture volume, ΔM_{fi} in equation (7) is zero; that is,

$$0 = M_{ti} + M_{Ii} + M_{Pi} \tag{9}$$

Since M_{I3} and M_{P3} are calculated by the formate concentration in the injection and production fluids, the net mass transfer M_{t3} can be obtained by equation (9).

To see the effectiveness of the formate imbibition into the matrix volume, the apparent imbibed fraction of component i (F_i) given as

$$F_i = \frac{-M_{ti}}{M_{Ii}} \tag{10}$$

represents the fraction of component i that is transferred from the fracture volume to the matrix volume. F_1 is the imbibed fraction of brine and F_3 is the imbibed fraction of formate. F_2 is not important because no oil was injected in the experiment.

The average concentration (weight percent) of the formate component in aqueous phase in the matrix volume can be calculated as

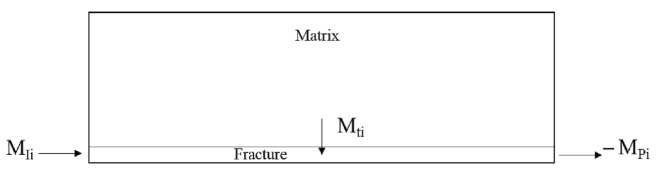

Fig. 5. Schematic for the mass balance analysis for dynamic imbibition with a fractured core.

$$w_m = \frac{-M_{t3}}{-M_{t1} - M_{t3} + M_{i1}} \quad (11)$$

where M_{i1} is the mass of initial water in the core. The summation of M_{t1}, M_{t3} and M_{i1} is the total mass of aqueous phase in matrix. This parameter is calculated on the cumulative base. The apparent concentration of formate in the imbibed water phase can be obtained by

$$w_f = \frac{M_{t3}}{M_{t1} + M_{t3}} \quad (12)$$

Note that this is also an "apparent" concentration because components 1 and 3 transfer independently between the two sub-volumes. These parameters help analyze the transfer of components as will be discussed in the Results section.

3. Results and discussion

3.1. Stability test

Fig. 6 shows the histories of solution pH values during the stability test. The 20 wt% formate solution showed a nearly constant pH value around 7 for more than 30 days, indicating that there was no reaction occurring within the solution. The other two solutions with calcite showed the equilibrium pH value near 9, indicating the calcite dissolution that caused bicarbonate (HCO_3^-) and increased the solution pH.

No precipitation was observed in the solutions with and without calcite during the entire aging period at 85 °C, indicating the stability of the formate solutions tested. Fig. 7 shows that the calcite powder was consumed more in the 20 wt% formate solution than in the brine during the stability test. Note again that the same amount of calcite was added to these two solutions in the preparation process. This result indicates that calcite dissolution occurs in the 20 wt% formate solution more than in the NaCl brine, starting at a neutral pH as shown in Fig. 6.

3.2. Wettability alteration test

Fig. 8 shows calcite plates during the wettability alteration test. For the brine case, no obvious change of the surface oil was observed after 6 days of immersion. The calcite surface was still oil-wet, indicating that brine was not effective in altering the wettability. For the calcite plate that was immersed in 30 wt% formate solution, however, the color of the calcite plate became lighter in some parts after 6 days. The wettability alteration by 30 wt% formate solution was more rapid than the wettability alteration by 5 wt% formate + HCl, as indicated by the color of the calcite surface. No change on the calcite plate surface was observed for 5 wt% formate. Results indicate that a higher concentration of formate led to more rapid calcite dissolution and therefore, wettability alteration.

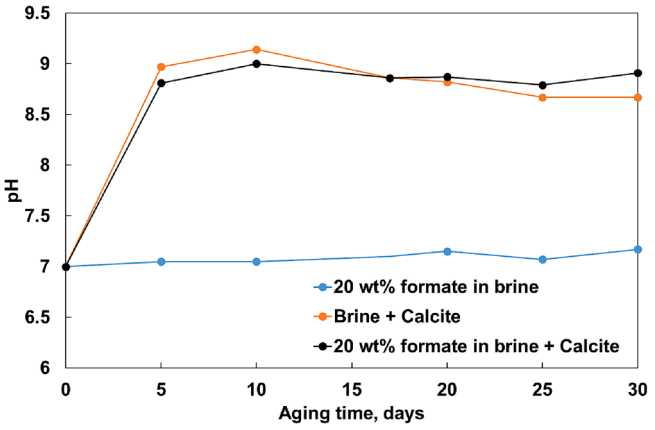

Fig. 6. Solution pH values during the stability test for the 20 wt% formate solution in the NaCl brine with and without calcite and the brine with calcite.

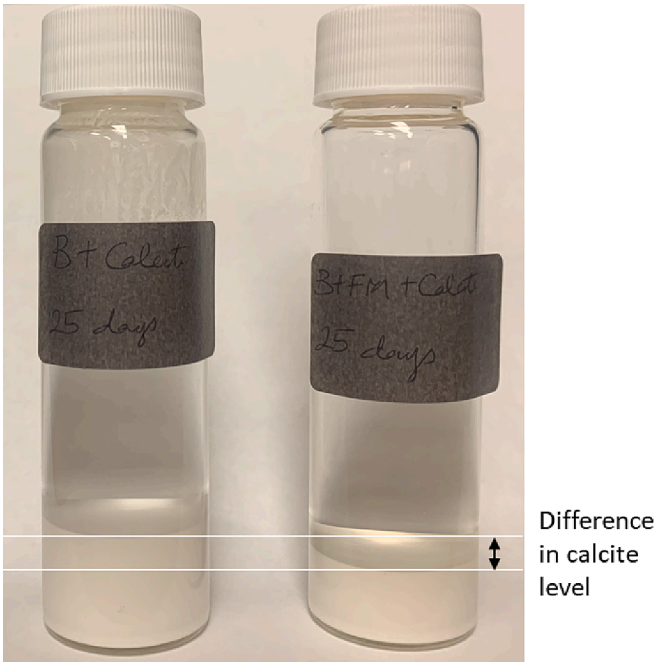

Fig. 7. Calcite powder was consumed more in the 20 wt% formate solution (right) than in the NaCl brine (left) during the stability test at 85 °C.

Fig. 9 shows the results of wettability alteration test with cores. No oil was observed on the top surface of the core in brine, but oil was recovered from the top surface for the other three formate cases. On day 6, a certain amount of oil was produced from the cores only in formate solutions, and the brine case almost remained the same as day 0. This indicates that formate was effective in altering wettability of the oil-wet porous media. The kinetics of wettability alteration for 30 wt% formate solution was much faster than 5 wt% formate + HCl solution, which in turn was faster than 5 wt% formate solution. Although Baghishov et al. [31] suggested using formate solution at a reduced pH by HCl for wettability alteration of oil-wet carbonate rocks, such a reduced pH was not required for 30 wt% formate solution to exhibit the wettability alteration. The solution pH affects the concentration of formate ion, and based on Equation (1) the formate concentration is 8.88 mol/L for 30 wt % formate solution with a pH of 7 and 1.18 mol/L for 5 wt% formate solution with a pH of 6.

During the wettability alteration test, CO_2 bubbles were observed on the surface of cores, as shown in Fig. 10. CO_2 bubbles were also observed on the side surface for 5 wt% formate + HCl and 30 wt% formate case in Fig. 9. However, no bubble was found for the brine case. Such CO_2 bubbles were produced where oil came out of the core, indicating the oil production by wettability alteration induced by calcite dissolution.

3.3. Dynamic imbibition and material balance

3.3.1. Coreflood #1 (30 wt% formate at a pH of 7)

Fig. 11 shows the oil recovery factor and pH of effluent samples for coreflood #1. The brine was injected into the core for 1.07 pore volumes (PVs), which was followed by the 30 wt% formate stage for 1.04 PVs. Finally, 1.54 PVs of chase brine was injected until the end of the experiment.

The oil recovery at the end of the brine stage was 12.9 %. In this stage, the water breakthrough occurred before 0.08 PVI because brine was displacing oil in the fracture, the volume of which was smaller than the pore volume. The pH of effluent samples fluctuated between 7.3 and 7.6 as the calcite dissolution was not significant with the injected brine.

The oil recovery increased rapidly at the beginning of the formate

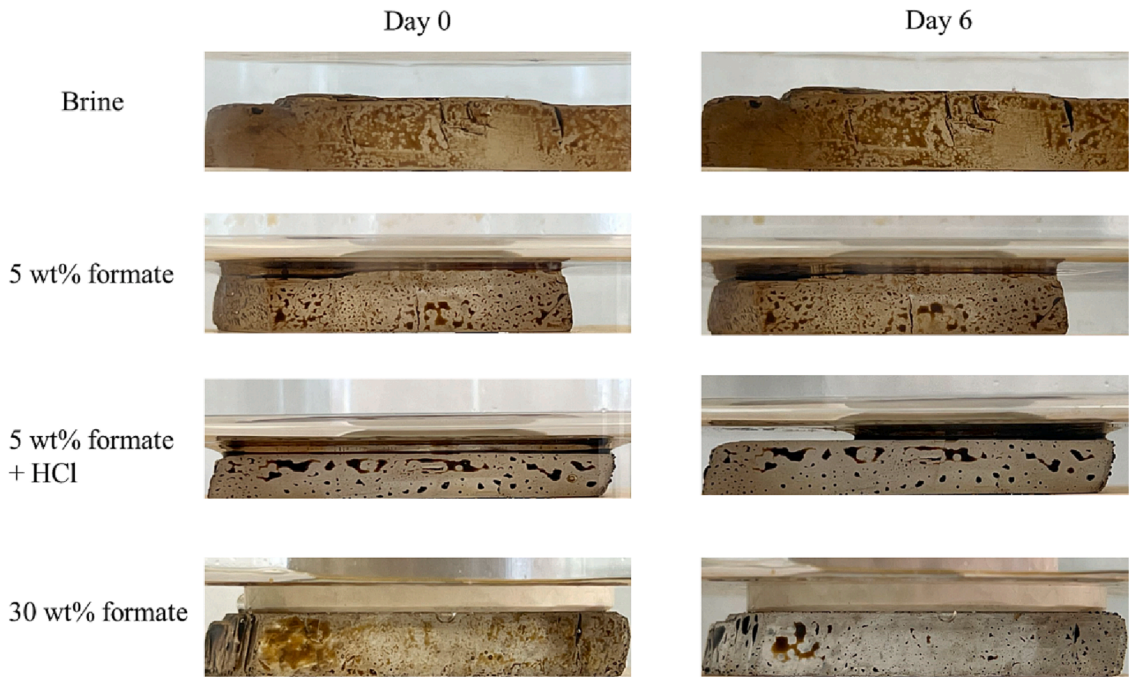

Fig. 8. Wettability alteration test with calcite plates on day 0 and day 6.

solution stage, indicating the water imbibition expelling oil from the matrix volume. The pH of effluent samples increased from 7.4 to 8.6 and leveled off below the equilibrium pH shown in Section 3.1. Note again that the pH of the injected formate solution was adjusted to 7 according to equation (1). Therefore, the increased pH was a result of the calcite dissolution in response to the formate solution injection. The oil recovery kept increasing until the formate injection was terminated. The incremental oil recovery for the formate stage was 6.8 %.

The oil recovery factor continued to increase in the initial part of the chase brine stage. Then, the ultimate incremental oil recovery was 9.1 %. The pH of effluent samples decreased gradually until the experiment was terminated.

Fig. 11 indicated that the injection of 30 wt% formate solution produced much more oil than the brine injection. Among several potential mechanisms, previous sections suggested wettability alteration induced by calcite dissolution should have caused the enhanced oil recovery by this highly concentrated formate solution. Note that Baghishov et al. [31] studied only 5 wt% formation solutions with and without HCl for adjusting the solution pH as described in the introduction section.

Fig. 12 shows the concentration of calcium in the effluent samples measured by ICP-MS for coreflood #1. The average concentration of calcium in the brine stage was about 47 ppm, whereas it increased significantly to 840 ppm in the formate solution stage. This result supports the occurrence of calcite dissolution during coreflood #1. The concentration of calcium during the formate stage was 18 times as large as that in brine stage. Even in the chase brine stage, the concentration of calcium was still as high as 695 ppm.

Fig. 13 shows the apparent imbibed fraction of brine (component 1) and formate (component 3). For the brine stage, a small amount of brine transferred from the fracture to the matrix according to the initial wetting state of the matrix. The oil in the matrix was expelled by the imbibed brine because of the volume balance in the matrix. However, the brine imbibition diminished with the continued brine injection (F_1 was 0.006). For the formate stage, formate began to transfer from the fracture to the matrix (F_3 was high at the beginning). This rapid imbibition of formate occurred likely because a large concentration gradient existed between the two sub-volumes. F_3 remained high during the formate solution stage and decreased to 0.15 after 1 PVI of formate solution. F_1 in the formate solution stage was evidently greater than that in the brine stage, which indicated that the water imbibition was enhanced by formate. For the chase brine stage, brine continued to be imbibed as F_1 was still about 0.05.

The amount of injected and produced formate were calculated to show the formate retention in the core. Baghishov et al. [31] reported the adsorption of formate in a Texas Cream limestone was 0.11 mg per gram of rock. Fig. 14 illustrates the accumulation of formate for coreflood #1. The retention of formate in the core was 1.54 g at the end of coreflood #1, which was much greater than 0.0216 g, the amount of adsorption using the mass of the dry core, 196.4 g. This result confirmed the mass transfer of formate between the fracture and matrix sub-volumes. A significant amount of formate retained in the matrix, which was desirable for carbon storage when the formate solution was used as an aqueous carbon carrier.

Fig. 15 illustrates the average formate concentration in the matrix volume for coreflood #1. The concentration of formate increased steadily after the formate stage started because of the efficient mass transfer as previously stated. This efficient transfer of formate into the matrix volume is advantageous when formate solution is injected for geological carbon storage. It reached a maximum of 23.5 wt% in coreflood #1. Even after the chase brine stage, the average concentration of formate in the matrix was still 8 wt%. This result was consistent with the large amount of retention as shown in Fig. 14.

Fig. 16 shows the apparent concentration of formate in the imbibed water for coreflood #1. Note again that this was an apparent value because it was calculated using the net transfer of formate and brine. Fig. 16 indicates that the maximum apparent concentration reached more than 60 wt%, which was far more than the solubility of formate in brine. Hence, water transferred not only from the fracture to the matrix sub-volume, but also in the opposite direction. The transfer of water from the matrix (low salinity) to the fracture volume (high salinity) is often called osmosis in the literature, in which oil is viewed as the semi membrane that water could pass through, but chemicals could not [40,41].

3.3.2. *Coreflood #2 (5 wt% formate at a pH of 7)*

Fig. 17 shows the oil recovery factor and pH of effluent samples for coreflood #2. The NaCl brine was injected for 1.03 PV, and then 5 wt%

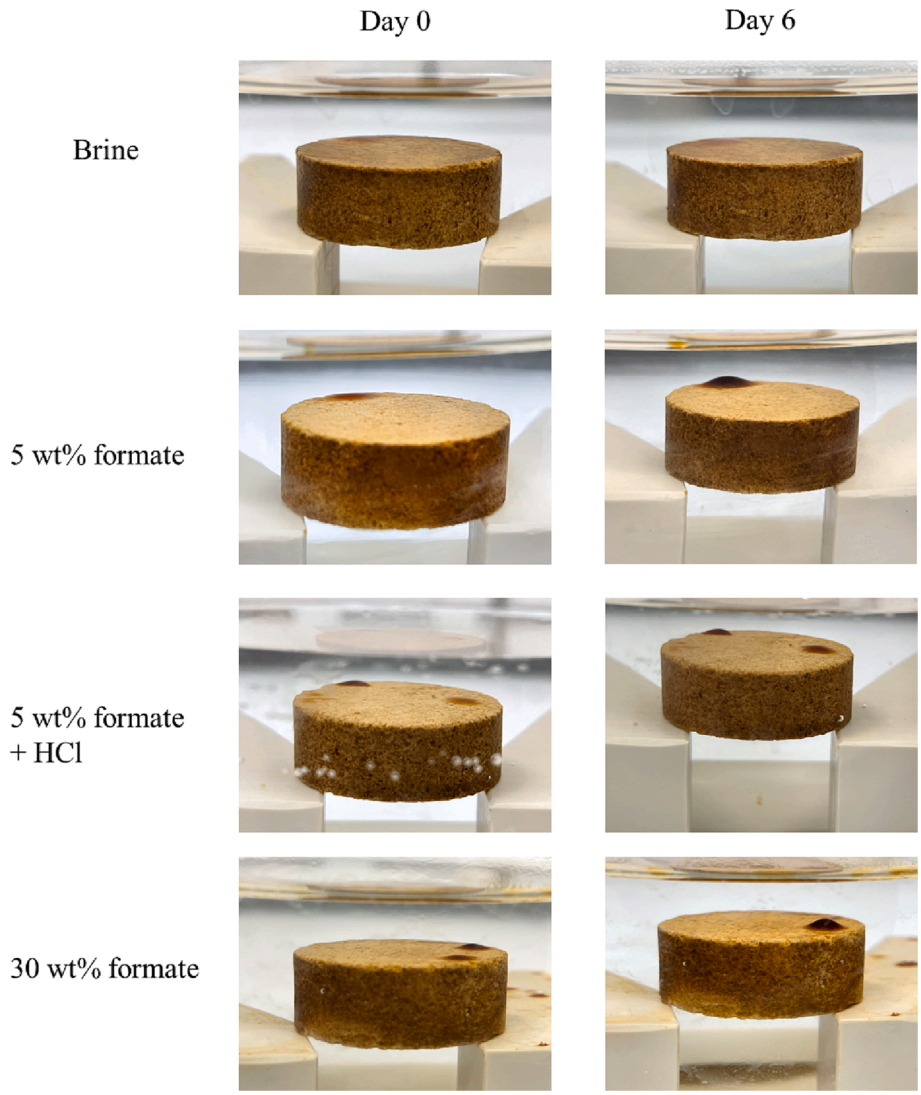

Fig. 9. Wettability alteration test with cores on day 0 and day 6. The bubbles shown in the photo of 5 wt% formate + HCl solution on day 0 were air bubbles generated during the preparation of experiment. They were removed carefully by needle on day 4.

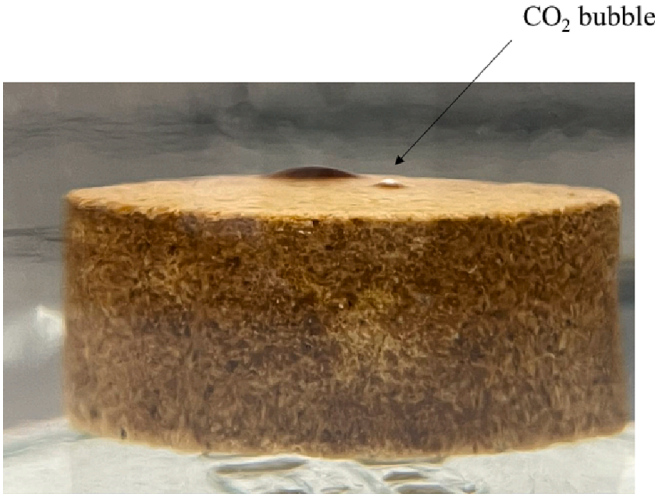

Fig. 10. CO_2 bubble produced in the wettability alteration test.

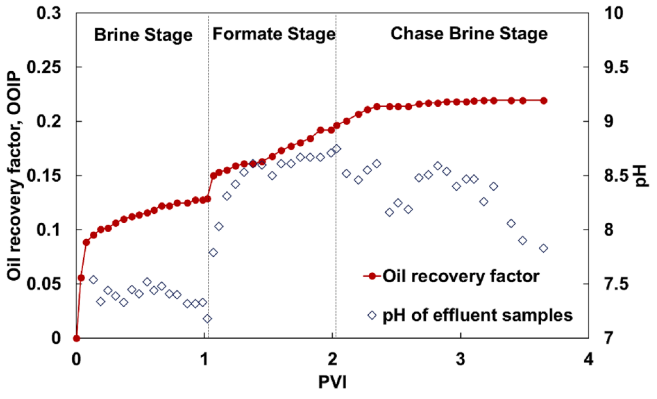

Fig. 11. Oil recovery factor and pH of effluents for coreflood #1.

formate solution for 1.03 PV. Finally, the chase brine was injected for 0.48 PV until no more oil was produced.

The oil recovery at the end of brine stage was 10.3 %, which was slightly smaller than coreflood #1. The pH values of effluent samples ranged between 7.1 and 7.4, which were close to the values in the brine

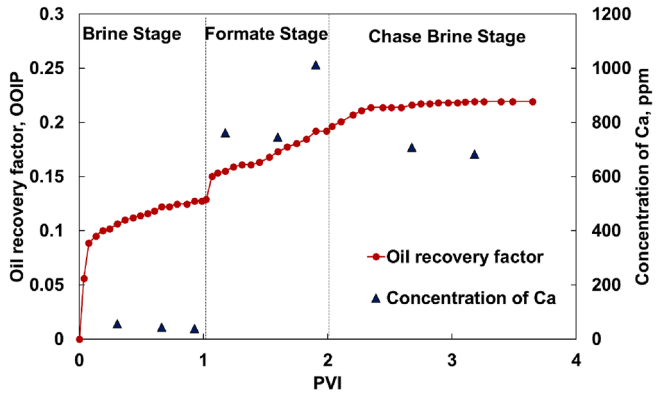

Fig. 12. Oil recovery factor and concentration of calcium for coreflood #1.

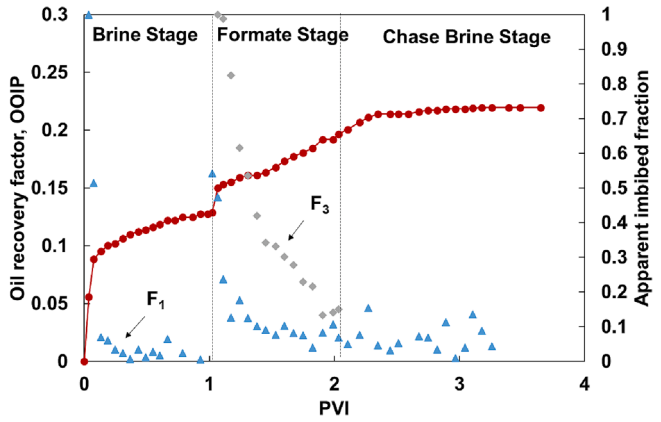

Fig. 13. Oil recovery factor and apparent imbibed fraction of brine (component 1) and formate (component 3) for coreflood #1.

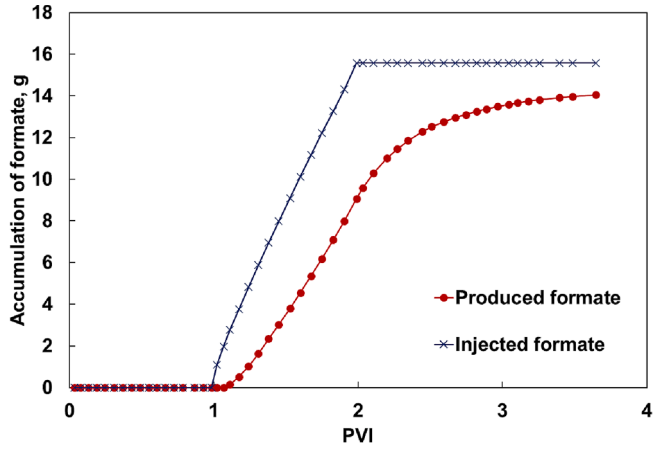

Fig. 14. The accumulation of injected and produced formate for coreflood #1.

stage for coreflood #1.

The formate solution stage showed a sudden increase in oil recovery at the beginning as was the case with coreflood #1. This confirmed that the water imbibition drove out the oil from the matrix upon the injection of the formate solution. The pH of effluent samples increased from 7.3 to 8.1 and reached a plateau, which was close to the reported value with 5 wt% formate from Baghishov et al. [31]. The oil recovery stopped increasing after 0.59 PVI of the formate solution. The pH of effluent samples decreased gradually in the chase brine stage until the experiment was terminated. The final incremental oil recovery for coreflood

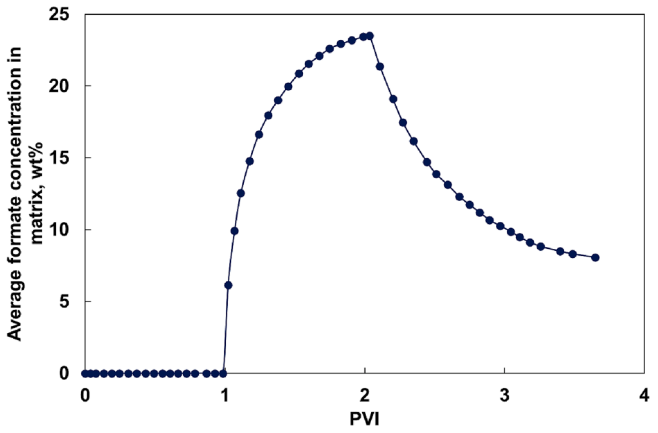

Fig. 15. .Average concentration of formate in the matrix for coreflood #1.

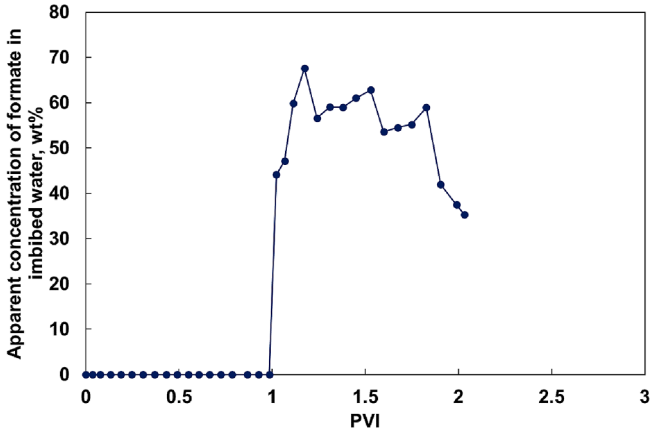

Fig. 16. Apparent concentration of formate in the imbibed water for coreflood #1.

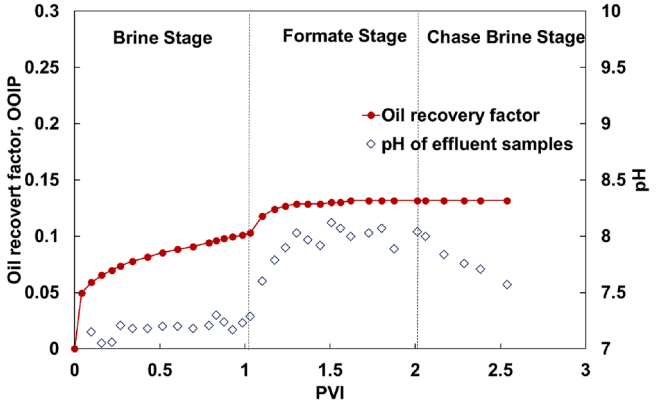

Fig. 17. Oil recovery factor and pH of effluents for coreflood #2.

#2 was 2.9 %. In this coreflood case, the calcite dissolution seemed to be weak because of the low concentration of formate; therefore, the incremental oil recovery was much smaller than coreflood #1.

The weaker calcite dissolution in coreflood #2 was supported by the measured concentrations of calcium in effluent samples as shown in Fig. 18. The concentration of calcium in the selected sample from the brine stage was 28 ppm, which was close to that for coreflood #1. The concentration of calcium in the formate solution stage increased gradually to 222 ppm, which was much smaller than 840 ppm in coreflood #1 (Fig. 12).

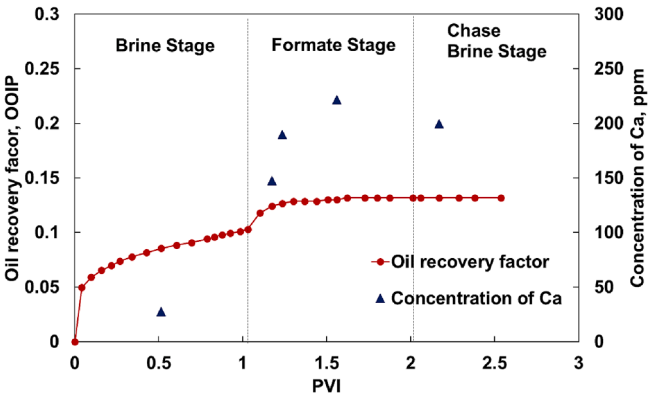

Fig. 18. Oil recovery factor and concentration of calcium for coreflood #2.

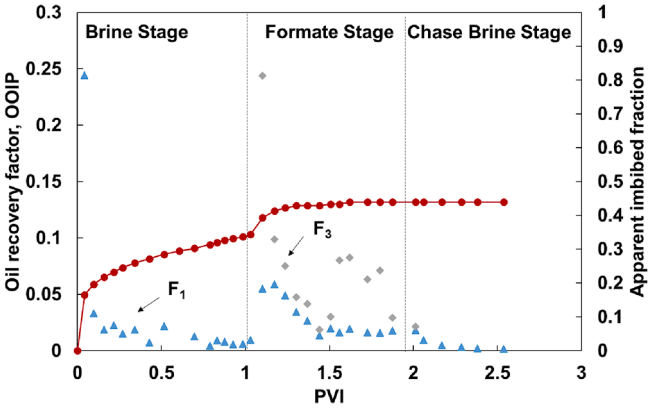

Fig. 19. Oil recovery factor and apparent imbibed fraction of brine and formate for coreflood #2. Note that the volumes of effluent samples were much smaller than expected from the injection rate after 1.5 PVI because of the water evaporation from the effluent samples. Therefore, the volume of water in effluents was obtained by the volume balance, the difference between the injected volume and the produced oil volume.

Fig. 19 shows the apparent imbibed fractions of brine (component 1) and formate (component 3). For the brine stage, the mass transfer behavior was similar to coreflood #1 with F_1 of 0.02. For the formate solution stage, F_3 was much smaller than that in coreflood #1 at the beginning. This was expected because the concentration gradient of formate was not as high as coreflood #1. F_3 increased between 1.56 and 1.88 PVI while F_1 was below 0.1, possibly because of the transient driving force, e.g., the formate concentration gradient between the matrix and fracture volumes. F_3 decreased to 0.07 after 1 PVI of formate solution. F_1 in the formate solution stage was still greater than that in the brine stage, but decreased rapidly after 1.17 PVI. Hence, the water imbibition was enhanced, although the effect was much limited. For the chase brine stage, F_1 was close to 0, which indicated the water imbibition diminished.

Fig. 20 shows the accumulation of formate for coreflood #2. The retention of formate in the core was 0.13 g at the end of coreflood #2, which was greater than 0.0192 g, the amount of adsorption using the mass of the dry core, 174.95 g. The retention of formate in this case was much smaller than that in coreflood #1 because of the limited mass transfer between the fracture and the matrix sub-volumes. Fig. 21 illustrates the average formate concentration in the matrix for coreflood #2. The maximum concentration of formate was 2.49 wt%, but it decreased to 1.29 wt% at the end of this experiment. Baghishov et al. [31] concluded that the wettability alteration of 5 wt% formate solution was ineffective without pH adjustment by HCl, which was consistent with results in this section.

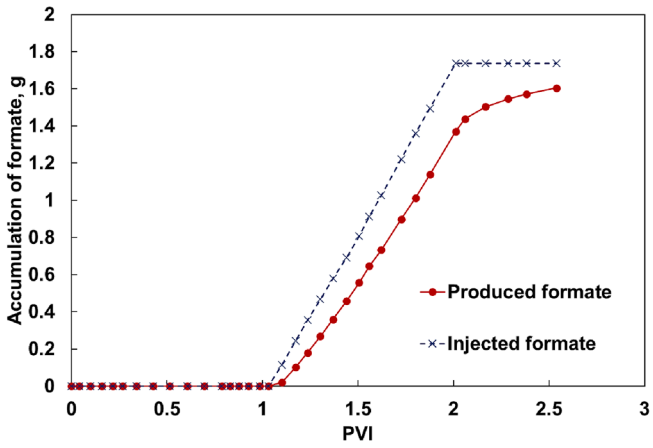

Fig. 20. The formate accumulation for coreflood #2.

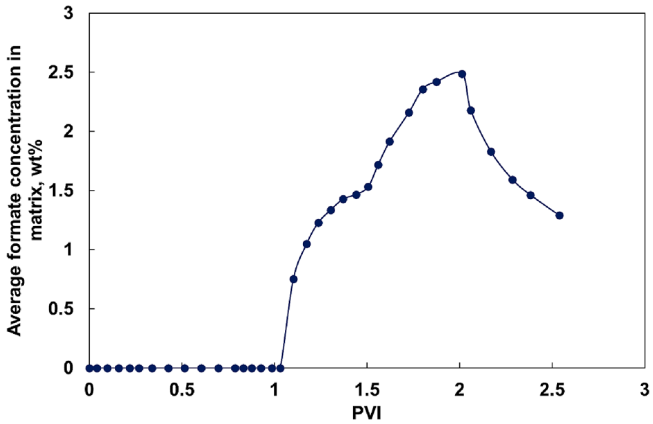

Fig. 21. The average formate concentration in the matrix for coreflood #2.

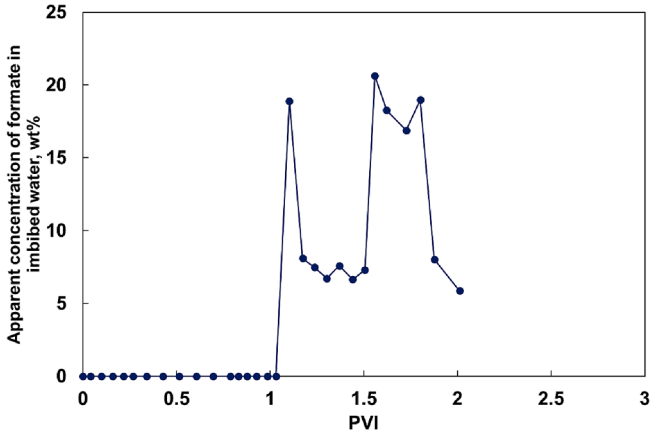

Fig. 22. Apparent concentration of formate in the imbibed water for coreflood #2.

Fig. 22 shows the apparent concentration of formate in the imbibed water for coreflood #2. The apparent concentration reached 20 wt% because the transfer of brine from the matrix to the fracture sub-volume also existed as discussed in the previous section. Again, the great apparent concentrations between 1.56 and 1.88 PVI were consistent with the values of F_3 in Fig. 19. The apparent concentration was only 5.87 wt% at the end of the formate solution stage likely because of the weaker wettability alteration.

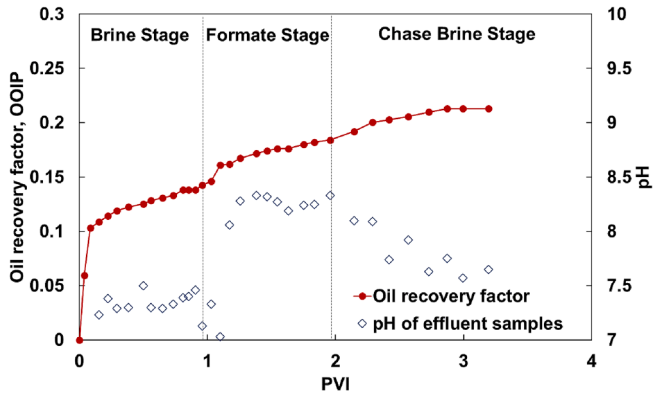

Fig. 23. Oil recovery factor and pH of effluents for coreflood #3.

3.3.3. *Coreflood #3 (5 wt% formate at a pH of 6)*

Fig. 23 shows the oil recovery factor and pH of effluent samples for coreflood #3. The NaCl brine was injected for 0.96 PVs, and then the formate solution was injected for 1.05 PVs. Finally, the chase brine was injected for 1.24 PVs until the end of the experiment.

The oil recovery at the end of the brine stage was 14.3 %. The pH of effluent samples ranged between 7.2 and 7.5. The formate solution stage showed a rapid increase in oil recovery at the beginning similarly to the other corefloods, and the pH of effluent samples increased from 7.4 and leveled off around 8.3. The stabilized pH was slightly greater than that in coreflood #2, which resulted from more calcite dissolution during the formate solution stage. Unlike in coreflood #2, however, the oil recovery kept increasing until the formate solution injection was terminated. The incremental oil recovery for the formate solution stage was 4.1 %.

The oil recovery factor continued to increase in the chase brine stage, indicating that brine continued to be imbibed into the matrix subvolume. The ultimate incremental oil recovery was 7.0 % in coreflood #3. The pH of effluent samples decreased gradually until the experiment was terminated.

As shown in Fig. 24, the concentration of calcium in the brine stage, 46 ppm, was close to the concentrations in the other two corefloods. It then increased to 281 ppm in the formate solution stage, which was greater than that for coreflood #2, but much smaller than that for coreflood #1. The effluent calcium concentrations are positively correlated with the incremental oil recovery factors in the three experiments.

Fig. 25 presents the apparent imbibed fraction of brine (component 1) and formate (component 3). F_1 gradually decreased until the end of the brine stage, and then increased to 0.28 in the formate solution stage, indicating the enhanced water imbibition by formate. F_3 was 0.11 in the formate solution stage and was 0.1 after 1 PVI of formate solution; that is, formate still transferred into the matrix and recovered oil from the matrix. In the chase brine stage, F_1 was 0.1 and brine continued to be

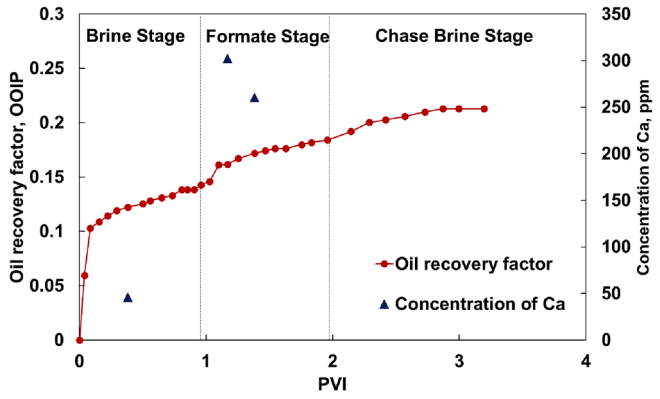

Fig. 24. Oil recovery factor and concentration of calcium for coreflood #3.

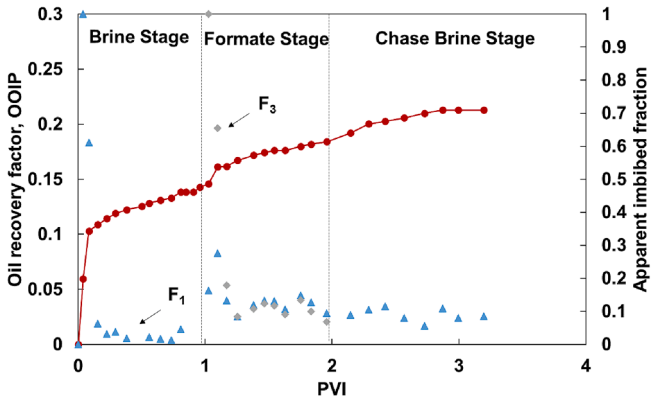

Fig. 25. Oil recovery factor and apparent imbibed fraction of brine and formate for coreflood #3.

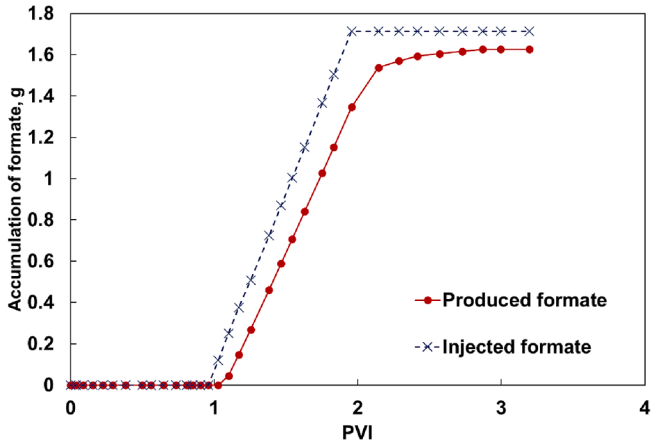

Fig. 26. Cumulative amounts of the injected and produced formate for coreflood #3.

imbibed into the matrix, resulting in the gradual oil recovery.

Fig. 26 presents the formate accumulation during coreflood #3 by the gap between the two curves. The retention of formate in the core was 0.087 g at the end of the experiment, which was greater than 0.022 g, the amount of adsorption using the mass of the dry core, 201.88 g. The retention of formate in this case was slightly smaller than coreflood #2 because a larger amount of chase brine was injected for coreflood #3 although they used the same formate concentration, 5 wt%. As shown in Fig. 27, the formate concentration reached 2.1 wt%, and then decreased to 0.41 wt% at the end of this experiment. Although the formate

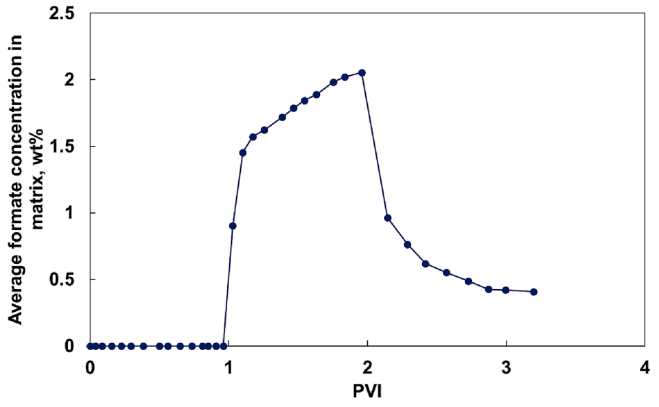

Fig. 27. Average formate concentration in the matrix for coreflood #3.

concentration in the matrix in coreflood #3 was as low as that in coreflood #2, coreflood #3 resulted in a greater oil recovery factor likely because the reduced pH by HCl contributed to the wettability alteration, as Baghishov et al. [31] showed in their paper.

Fig. 28 shows the apparent concentration of formate in the imbibed water for coreflood #3. It reached 20 wt% and then decreased to 3.5 wt %. Similarly, the transfer of water from the matrix to fracture volume also existed as discussed before. The apparent concentration was stable after 1.2 PVI, indicating a stable water imbibition from fracture and matrix.

3.4. Discussion

This section discusses the comparison among the three corefloods given in the previous section. The comparison is focused on the effects of formate concentration and solution pH on wettability alteration.

3.4.1. Scaling oil recovery curves

Fig. 29 (a) compares the oil recovery behavior of three corefloods in terms of PVI. Since the three corefloods used different cores, the oil recovery curves needed to be scaled. Although there are mathematical models for dynamic imbibition (e.g. [42]), a proper scaling process required many parameters, some of which were not available in this research. Because the injection flow rates into the fracture volume were small, a scaling equation for static imbibition was used [43]. This scaling equation was originally proposed for strongly water-wet systems, but Mirzaei-Paiaman et al. [44] showed its applicability to other wetting states, for example, mixed wet rocks. Note that the three coreflood tests were comparable in terms of injection flow rate, system geometry, and fracture properties. This further supports use of this static imbibition scaling equation as

$$t_{D-MFMR} = t\sqrt{\frac{k}{\varphi}}\,\frac{\sigma}{L_c^2}\,\frac{2}{\mu_w + \sqrt{\mu_w \mu_o}} \tag{13}$$

where t is the imbibition time, k is the matrix permeability, φ is the matrix porosity, σ is the interfacial tension between oleic and aqueous phase, μ_w is the viscosity of the water phase, and μ_o is viscosity of the oil phase. L_c is characteristic length

$$L_c = \sqrt{\frac{V_b}{\sum_{i=1}^{n} \frac{A_i}{l_{A_i}}}} \tag{14}$$

where V_b is the matrix bulk volume, A_i is the i-th surface area that is open to imbibition, and l_{A_i} is the distance from the i-th surface to the no-flow boundary.

The scaled oil recovery curve is shown in Fig. 29 (b). Coreflood #1 gave the fastest oil recovery. The oil recoveries at the end of corefloods #1 and #3 were clearly higher than that of coreflood #2, indicating the wettability alteration in these two cases.

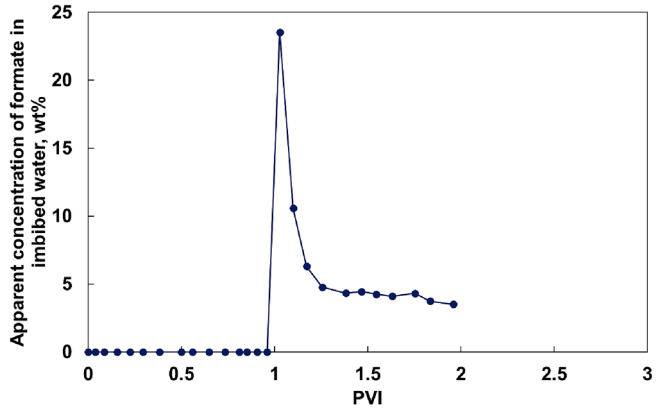

Fig. 28. Apparent formate concentration in the imbibed water for coreflood #3.

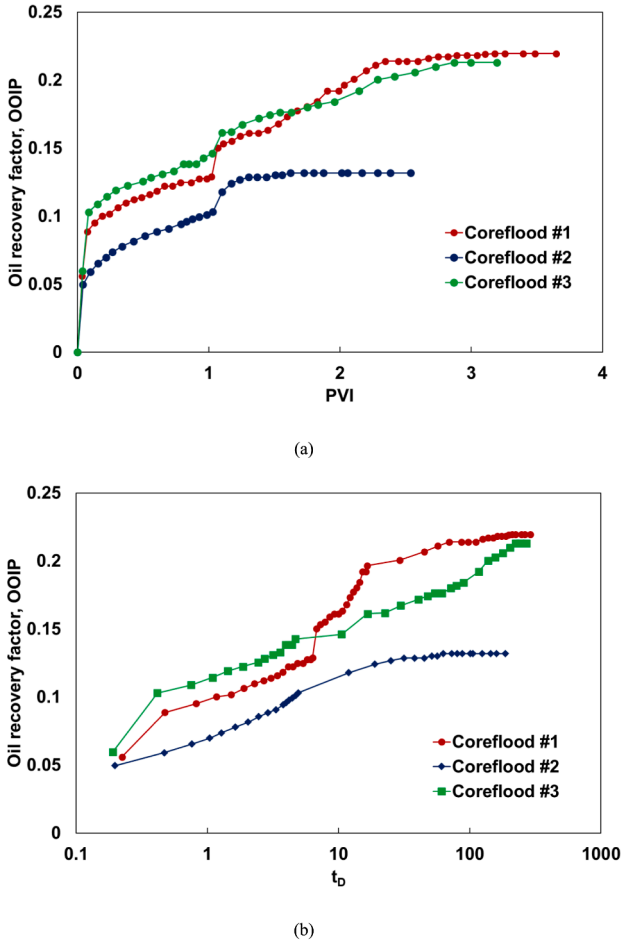

Fig. 29. Comparison of oil recovery for three corefloods in terms of (a) PVI and (b) dimensionless time.

3.4.2. Effect of formate concentration

Figs. 11 and 17 show that coreflood #1 yielded a much greater oil recovery factor than coreflood #2. The solution pH in the formate solution stage was 8.6 for coreflood #1 and 8.1 for coreflood #2. The calcium concentration at the effluent was 840 ppm in coreflood #1 and 222 ppm in coreflood #2. These results make it reasonable to conclude that a greater formate concentration contributed to a greater level of calcite dissolution and wettability alteration, which in turn enhanced the water imbibition to expel the oil from the matrix sub-volume.

At the end of the formate solution stage, F_3 was 0.15 for coreflood #1 and 0.07 for coreflood #2. F_1 increased to 0.54 for coreflood #1 at the beginning of formate stage, which was much greater than 0.18 for coreflood #2. That is, the mass transfer of formate and brine between the fracture and the matrix sub-volumes was more effective with a greater concentration of formate. Consequently, a greater concentration of formate resulted in a greater level of retention of formate in the matrix, which contributes to geological carbon storage if formate is viewed as a carbon carrier.

The concentration of formate in the matrix cannot be greater than that in the injected fluid; hence, the average formate concentration in the matrix was only 2.49 wt% at most in coreflood #2 as shown in Fig. 21. This concentration is less than a half of the concentration in the injected fluid, 5 wt%. This is consistent with Baghishov et al. [31] who concluded that 5 wt% formate solution with no pH adjustment did not

have a clear impact on calcite wettability.

3.4.3. Effect of pH

The only difference between corefloods #2 and #3 is the solution pH: 7 for coreflood #2 and 6 for coreflood #3. The oil recovery factor was greater in coreflood #3 than in coreflood #2 (Figs. 17 and 23). The pH at the end of the formate solution stage was 8.1 for coreflood #2 and 8.3 for coreflood #3. The calcium concentration in effluent samples was 222 ppm for coreflood #2 and 281 ppm for coreflood #3. Hence, a reduced pH in the injected formate solution contributed to a greater level of calcite dissolution, enhancing the water imbibition. F_1 and F_3 for two cases were close to each other, indicating the mass transfers between fracture and matrix were similar.

Increasing the concentration of H^+ moved the calcite dissolution reaction so that calcite dissolution could be induced. As a result, a reduced pH of formate solution could yield a higher oil recovery factor if a low concentration of formate (e.g., 5 wt% as in Baghishov et al.[31]) was used.

3.4.4. Two potential mechanisms of wettability alteration by formate solution

Based on results from this research and Baghishov et al. [31], 5 wt% formate solution showed wettability alteration via a slightly increased level of calcite dissolution with a pH adjustment as quantified by the calcium concentrations at the effluent. However, results in this research suggested that wettability alteration by formate solution also occurs by an elevated concentration of formate even at a neutral pH. It is hypothesized that decreasing the initial solution pH induces calcite dissolution to increase the concentrations of HCO_3^- and Ca^{2+} in the solution, but increasing the formate concentration does so to increase the concentrations of formate species, such as $Ca(HCOO)_2$ and $Ca(HCOO)^+$ in the solution and adsorbed formate species on the rock surface. These species would not occur without adding formate to the solution. Fig. 30 schematically shows the aforementioned mechanism of wettability alteration by formate solution.

The substantial level of incremental oil recovery in coreflood #1 (Fig. 11) and the rapid imbibition of formate into the matrix (Fig. 15) indicate that formate can contribute as a wettability alteration agent for EOR and/or as a carbon carrier for geological carbon storage. Increasing the formate concentration is advantageous for both purposes.

4. Conclusions

The main conclusions of this paper are as follows:

1. The 20 wt% formate solution in 15000 ppm NaCl brine was stable at 85 °C with no change in pH for more than 30 days. The 20 wt% formate solution and the base NaCl brine showed essentially the same pH history with calcite powder, where calcite dissolution caused the solution pH to increase to a stable value near 9. However, the amount of dissolved calcite was greater with 20 wt% formate than without formate in the bottle tests at 85 °C. None of the samples studied in this research showed solid precipitation.
2. The wettability alteration experiments showed that formate solutions could change the wettability of calcite plates to a more water-wet state and result in more oil recovery as also confirmed in corefloods.
3. Material balance of coreflooding data indicated that water imbibition into the matrix was enhanced by the formate solution injection, and therefore, part of the oil in the matrix was expelled and produced. The imbibition of formate into the matrix was most significant in coreflood #1. A large gradient in formate concentration from the fracture to the matrix sub-volume likely caused the rapid mass transfer. Calcite dissolution was caused by the increasing formate

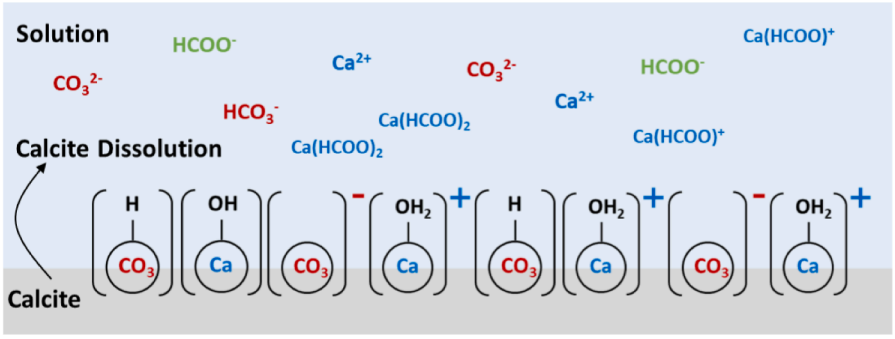

(a)

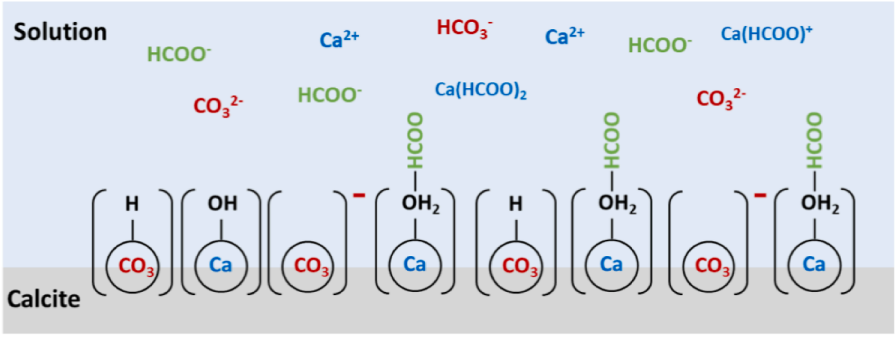

(b)

Fig. 30. Wettability alteration mechanism by formate solution: (a) Calcite dissolution induced by an elevated formate concentration and/or decreased pH and (b) wettability alteration by the adsorption of formate on the rock surface.

concentration, and then, formate species in the matrix acted as the wettability modifier to enhance water imbibition, which in turn expelled the oil in the matrix.

4. The mechanisms of wettability alteration by formate solution include calcite dissolution as confirmed by elevated concentrations of calcium at the effluent in the formate solution injection stage for three dynamic imbibition experiments. We showed for the first time that wettability alteration involving calcite dissolution can occur at a neutral pH of 7 with an elevated concentration of formate.
5. The incremental oil recovery factor was 9.1 % for 30 wt% formate (pH = 7), 2.9 % for 5 wt% formate (pH = 7), and 7.0 % for 5 wt% formate + HCl (pH = 6). A greater oil recovery factor resulted from a greater concentration of formate and a reduced pH.

CRediT authorship contribution statement

Hao Wang: Methodology, Validation, Formal analysis, Investigation, Data curation, Writing – original draft, Visualization. **Oluwafemi Precious Oyenowo:** Methodology, Validation, Formal analysis, Investigation, Data curation. **Ryosuke Okuno:** Conceptualization, Methodology, Validation, Formal analysis, Resources, Writing – review & editing, Supervision, Project administration, Funding acquisition.

Declaration of Competing Interest

The authors declare that they have no known competing financial interests or personal relationships that could have appeared to influence the work reported in this paper.

Data availability

Data will be made available on request.

Acknowledgement

We acknowledge the support of JX Nippon Oil & Gas Exploration for this research along with sponsors of the Energi Simulation Industrial Affiliate Program on Carbon Utilization and Storage (ES Carbon UT) at the Center for Subsurface Energy and The Environment at the University of Texas at Austin. Ryosuke Okuno holds the Pioneer Corporation Faculty Fellowship in the Hildebrand Department of Petroleum and Geosystems Engineering at The University of Texas at Austin.

References

[1] Alotaibi, M. B., Nasralla, R. A., & Nasr-El-Din, H. A. (2010, April). Wettability Challenges in Carbonate Reservoirs. SPE Improved Oil Recovery Symposium. 10.2118/129972-MS.
[2] Agar SM, Geiger S. Fundamental Controls on Fluid Flow in Carbonates: Current Workflows to Emerging Technologies. Geol Soc Lond Spec Publ 2015;406(1):1–59. https://doi.org/10.1144/SP406.
[3] Moritis G. Point of View: CO_2 Geological Sequestration Opens Opportunities for Permian Basin. Oil Gas J 2004;102(1):39–41.
[4] Mogensen K, Masalmeh S. A Review of EOR Techniques for Carbonate Reservoirs in Challenging Geological Settings. J Pet Sci Eng 2020;195:107889. https://doi.org/10.1016/j.petrol.2020.107889.
[5] Egermann P, Robin M, Lombard JM, Modavi A, Kalam MZ. Gas Process Displacement Efficiency Comparisons on a Carbonate Reservoir. SPE Reserv Eval Eng 2006;9(06):621–9. https://doi.org/10.2118/81577-PA.
[6] Tan Y, Li Q, Xu L, Ghaffar A, Zhou X, Li P. A Critical Review of Carbon Dioxide Enhanced Oil Recovery in Carbonate Reservoirs. Fuel 2022;328:125256. https://doi.org/10.1016/j.fuel.2022.125256.
[7] Alcorn, Z. P., Fernø, M. A., & Graue, A. (2020, May). Upscaling CO_2 Foam for EOR as CCUS from On-To Offshore. Offshore Technology Conference. 10.4043/30677-MS.
[8] Hassan, H., Omar, N. F. N., Jalil, A. A. M. M., Salihuddin, R. S., & Shah, S. S. M. (2018, March). Gearing toward CCUS for CO_2 reduction in Malaysia. Offshore Technology Conference Asia. 10.4043/28408-MS.
[9] Rodrigues HW, Mackay EJ, Arnold DP. Multi-objective Optimization of CO_2 Recycling Operations for CCUS in Pre-salt Carbonate Reservoirs. Int J Greenhouse Gas Control 2022;119:103719. https://doi.org/10.1016/j.ijggc.2022.103719.
[10] Alcorn, Z. P., Fredriksen, S. B., Sharma, M., Rognmo, A. U., Føyen, T. L., Fernø, M. A., & Graue, A. (2018, April). An Integrated CO_2 Foam EOR Pilot Program with Combined CCUS in an Onshore Texas Heterogeneous Carbonate Field. SPE Improved Oil Recovery Conference. 10.2118/190204-MS.
[11] Lv Q, Zheng R, Zhou T, Guo X, Wang W, Li J, et al. Visualization Study of CO_2-EOR in Carbonate Reservoirs Using 2.5 D Heterogeneous Micromodels for CCUS. Fuel 2022;330:125533. https://doi.org/10.1016/j.fuel.2022.125533.
[12] Talebian SH, Masoudi R, Tan IM, Zitha PLJ. Foam Assisted CO_2-EOR: A Review of Concept, Challenges, and Future Prospects. J Pet Sci Eng 2014;120:202–15. https://doi.org/10.1016/j.petrol.2014.05.013.
[13] Buckley JS. Effective Wettability of Minerals Exposed to Crude Oil. Curr Opin Colloid Interface Sci 2001;6(3):191–6. https://doi.org/10.1016/S1359-0294(01)00083-8.
[14] Hamon, G. (2004, September). Revisiting Ekofisk and Eldfisk Wettability. SPE Annual Technical Conference and Exhibition. 10.2118/90014-MS.
[15] Seethepalli, A., Adibhatla, B., & Mohanty, K. K. (2004, April). Wettability Alteration during Surfactant Flooding of Carbonate Reservoirs. SPE/DOE Symposium on Improved Oil Recovery. 10.2118/89423-MS.
[16] Hirasakl GJ. Wettability: Fundamentals and Surface Forces. SPE Form Eval 1991;6(02):217–26. https://doi.org/10.2118/17367-pa.
[17] Chen P, Mohanty KK. Surfactant-mediated Spontaneous Imbibition in Carbonate Rocks at Harsh Reservoir Conditions. SPE J 2013;18(01):124–33. https://doi.org/10.2118/153960-PA.
[18] Kalam S, Abu-Khamsin SA, Kamal MS, Patil S. A Review on Surfactant Retention on Rocks: Mechanisms, Measurements, and Influencing Factors. Fuel 2021;293:120459. https://doi.org/10.1016/j.fuel.2021.120459.
[19] Yao Y, Wei M, Kang W. A Review of Wettability Alteration using Surfactants in Carbonate Reservoirs. Adv Colloid Interface Sci 2021;294:102477. https://doi.org/10.1016/j.cis.2021.102477.
[20] Standnes DC, Nogaret LA, Chen HL, Austad T. An Evaluation of Spontaneous Imbibition of Water into Oil-wet Carbonate Reservoir Cores Using a Nonionic and a Cationic Surfactant. Energy Fuel 2002;16(6):1557–64. https://doi.org/10.1021/ef0201127.
[21] Salehi M, Johnson SJ, Liang JT. Mechanistic Study of Wettability Alteration Using Surfactants with Applications in Naturally Fractured Reservoirs. Langmuir 2008;24(24):14099–107. https://doi.org/10.1021/la802464u.
[22] Kathel P, Mohanty KK. Wettability Alteration in a Tight Oil Reservoir. Energy Fuel 2013;27(11):6460–8. https://doi.org/10.1021/ef4012752.
[23] Tang GQ, Morrow NR. Influence of Brine Composition and Fines Migration on Crude Oil/brine/rock Interactions and Oil recovery. J Pet Sci Eng 1999;24(2–4):99–111. https://doi.org/10.1016/S0920-4105(99)00034-0.
[24] Yildiz HO, Morrow NR. Effect of Brine Composition on Recovery of Moutray Crude Oil by Waterflooding. J Pet Sci Eng 1996;14(3–4):159–68. https://doi.org/10.1016/0920-4105(95)00041-0.
[25] Zhang, Y., Xie, X., & Morrow, N. R. (2007, November). Waterflood Performance by Injection of Brine with Different Salinity for Reservoir Cores. SPE Annual Technical Conference and Exhibition. 10.2118/109849-MS.
[26] Sheng JJ. Critical Review of Low-salinity Waterflooding. J Pet Sci Eng 2014;120:216–24. https://doi.org/10.1016/j.petrol.2014.05.026.
[27] Zhang P, Tweheyo MT, Austad T. Wettability Alteration and Improved Oil Recovery in Chalk: The Effect of Calcium in the Presence of Sulfate. Energy Fuel 2006;20(5):2056–62. https://doi.org/10.1021/ef0600816.
[28] Ligthelm, D. J., Gronsveld, J., Hofman, J., Brussee, N., Marcelis, F., & van der Linde, H. (2009, June). Novel Waterflooding Strategy by Manipulation of Injection Brine Composition. EUROPEC/EAGE Conference and Exhibition. 10.2118/119835-MS.
[29] Hiorth A, Cathles LM, Madland MV. The Impact of Pore Water Chemistry on Carbonate Surface Charge and Oil Wettability. Transp Porous Media 2010;85(1):1–21. https://doi.org/10.1007/s11242-010-9543-6.
[30] Den Ouden, L., Nasralla, R. A., Guo, H., Bruining, H., & Van Kruijsdijk, C. P. J. W. (2015, April). Calcite Dissolution Behaviour during Low Salinity Water Flooding in Carbonate Rock. IOR 2015-18th European Symposium on Improved Oil Recovery. https://doi.org/10.3997/2214-4609.201412102.
[31] Baghishov I, Abeykoon GA, Wang M, Oyenowo OP, Argüelles-Vivas FJ, Okuno R. A Mechanistic Comparison of Formate, Acetate, and Glycine as Wettability Modifiers for Carbonate and Shale Formations. Colloids Surf A Physicochem Eng Asp 2022;652:129849. https://doi.org/10.1016/j.colsurfa.2022.129849.
[32] Oyenowo OP, Sheng K, Okuno R. Simulation case studies of aqueous formate solution for geological carbon storage. Fuel 2023;334:126643. https://doi.org/10.1016/j.fuel.2022.126643.
[33] Okuno R (2022). Novel Fluids for Enhanced Carbon Storage. The 2022 Energi Simulation Summit. Calgary, Alberta, Canada. https://energisimulation.com/2022/09/15/novel-fluids-for-enhanced-carbon-storage-by-ryosuke-okuno.
[34] Rapoport, L. A., & Leas, W. J. (1953). Properties of Linear Waterfloods. Journal of Petroleum Technology, 5(05), 139-148. http:// doi.org/10.2118/213-G.
[35] Parra, J. E., Pope, G. A., Mejia, M., & Balhoff, M. T. (2016, September). New Approach for Using Surfactants to Enhance Oil Recovery from Naturally Fractured Oil-wet Carbonate Reservoirs. SPE Annual Technical Conference and Exhibition. 10.2118/181713-MS.
[36] Mejia, M. (2018, December). Experimental Investigation of Surfactant Flooding in Fractured Limestones. MS thesis, The University of Texas at Austin.
[37] Argüelles-Vivas FJ, Wang M, Abeykoon GA, Okuno R. Oil Recovery from Fractured Porous Media with/without Initial Water Saturation by Using 3-pentanone and Its Aqueous Solution. Fuel 2020;276:118031. https://doi.org/10.1016/j.fuel.2020.118031.

[38] Wang M, Abeykoon GA, Argüelles-Vivas FJ, Okuno R. Aqueous Solution of Ketone Solvent for Enhanced Water Imbibition in Fractured Carbonate Reservoirs. SPE J 2020;25(05):2694–709. https://doi.org/10.2118/200340-pa.
[39] Dai KK, Orr Jr FM. Prediction of CO_2 flood performance: Interaction of phase behavior with microscopic pore structure heterogeneity. SPE Reserv Eng 1987;2 (04):531–42. https://doi.org/10.2118/13115-PA.
[40] Torcuk, M. A., Uzun, O., Padin, A., & Kazemi, H. (2019, September). Impact of Chemical Osmosis on Brine Imbibition and Hydrocarbon Recovery in Liquid-rich Shale Reservoirs. SPE Annual Technical Conference and Exhibition. 10.2118/ 195909-MS.
[41] Takeda M, Manaka M, Ito D. Experimental Evidence of Chemical Osmosis-driven Improved Oil Recovery in Low-salinity Water Flooding: Generation of Osmotic Pressure via Oil-Saturated Sandstone. J Pet Sci Eng 2022;215:110731.
[42] Nia SF, Jessen K. Theoretical analysis of capillary rise in porous media. Transp Porous Media 2015;110(1):141–55. https://doi.org/10.1007/s11242-015-0562-1.
[43] Mason G, Fischer H, Morrow NR, Ruth DW. Correlation for the effect of fluid viscosities on counter-current spontaneous imbibition. J Pet Sci Eng 2010;72(1–2): 195–205. https://doi.org/10.1016/j.petrol.2010.03.017.
[44] Mirzaei-Paiaman A, Saboorian-Jooybari H, Masihi M. Incorporation of viscosity scaling group into analysis of MPMS index for laboratory characterization of wettability of reservoir rocks. J Pet Explor Prod Technol 2017;7:205–16. https:// doi.org/10.1007/s13202-016-0231-0.